Amorphous SiO_2/Si Interface Defects and Mechanism of Passivation/Depassivation Reaction

Hong Zhuocheng[1], *Zuo Xu*[1,2,3]

(1. College of Electronic Information and Optical Engineering, Nankai University, Tianjin 300350, China;
2. Key Laboratory of Photoelectronic Thin Film Devices and Technology of Tianjin, Tianjin 300350, China;
3. Engineering Research Center of thin film optoelectronics technology, Ministry of Education, Tianjin 300350, China)

Abstract: The amorphous silicon dioxide/silicon (a-SiO_2/Si) interface is an important part of semiconductor devices. The passivation and depassivation process of silicon dangling bond defects (P_b-type defects) at the SiO_2/Si interface has a significant impact on semiconductor devices. *Based on molecular dynamics and first-principles calculation methods, a-SiO_2/Si(111) interface model is constructed based on a-SiO_2 and crystalline Si. The CI-NEB (Climbing Image-Nudged Elastic Band) method is used to study the passivation and depassivation reactions of H_2 and H atoms of P_b defects at the a-SiO_2/Si(111) interface.* The curves, barriers, and transition state structures of the passivation and depassivation reactions based on the a-SiO_2/Si model are discussed.

Keywords: first-principles; a-SiO_2/Si(111) interface; passivation/depassivation; NEB method

非晶 SiO_2/Si 界面缺陷及其钝化/去钝化反应机制

洪卓呈[1]，左旭[1,2,3]

(1. 南开大学电子信息与光学工程学院，天津 300350；2. 天津市光电子薄膜器件与技术重点实验室，天津 300350；
3. 薄膜光电子技术教育部工程研究中心，天津 300350)

摘要：研究非晶二氧化硅/硅(a-SiO_2/Si)界面处的硅悬挂键缺陷(即 P_b 类缺陷)的钝化与去钝化过程对提高器件性能具有重要意义。*基于分子动力学与第一性原理计算方法，以 a-SiO_2 和晶体 Si 为基础，构建了 a-SiO_2/Si(111)界面模型。采用 CI-NEB (Climbing Image-Nudged Elastic Band)方法分别对 a-SiO_2/Si(111)界面的 P_b 缺陷分别于氢气和氢原子的钝化、去钝化反应进行了研究。*明确了基于非晶二氧化硅/硅界面缺陷模型的钝化、去钝化反应的反应曲线、反应势垒以及反应的过渡态结构。

关键词：第一性原理；a-SiO_2/Si(111)界面；钝化/去钝化；NEB 方法
中图分类号：TP391.9 文献标识码：A 文章编号：1004-731X (2020) 12-2362-14
DOI: 10.16182/j.issn1004731x.joss.20-FZ0474E

Introduction

With the wide application of Metal-Oxide-Semiconductor (MOS) technology in semiconductor devices, the Si/SiO_2 interface, which plays an important role in MOS technology, has also been widely studied. Previous studies have pointed out that hydrogen can exist in SiO_2 defects[1]. Ionizing radiation causes hydrogen-containing defects to release protons (H^+), and the H^+ "hops" through the

Received date:2020-03-20 Revised date: 2020-08-02; Foundation item: Science Challenge Project (TZ2016 003-1-105), CAEP Microsystem and THz Science and Technology Foundation (CAEPMT201501), National Basic Research Program of China (2011CB606405);
Biographies: Hong Zhuocheng (1996-), female, Guangxi, graduate student, research direction is SiO_2/Si interface defects and their passivation and depassivation mechanisms.

a-SiO_2 to reach the interface in the defects[2]. When the protons migrate to the interface, those defects which have been depassivatd will be reactivated, resulting in degradation of device performance[3].

Therefore, we need to study the process of passivation and depassivation to better understand the influence of protons or hydrogen atoms generated by ionizing radiation on interface defects.

Generally, silicon with threefold- coordinated at the a-SiO_2/Si interface is called the P_b defect[4]. Previous studies have shown that the configuration of P_b-type defects is $Si \equiv Si$ [5-7], that is, there is a Si dangling bond on the side near the Si in the interface. There are three types of defects in the interface, terming P_b, P_{b0}, and P_{b1} respectively, where P_b defects are located at the a-SiO_2/Si(111) interface[8-10], while P_{b0} and P_{b1} defects are located at the a-SiO_2/Si(100) interface[5-7,11]. In addition, the P_b defect and P_{b0} defect are along the [111] direction of the interface, while P_{b1} is along the [112] direction of the interface (the interface normal direction is along [100]).

Edwards used some finite cluster models to study EPR parameters, structural stability, and defect energy levels of Si/SiO_2 interface. However, because these cluster models are lack of universality, they cannot reflect the specific properties of the a-SiO_2/Si(111) interface[4].

Hyperfine parameters can reflect certain properties of defects[12]. Researchers can obtain experimental values through electron paramagnetic resonance(EPR).

Cook and White[13] considered valence polarization and nuclear polarization, and used the MS-Xα method to calculate the hyperfine parameters of defects in the P_b cluster model. In their study, they found that fermi contact (the isotropic interaction) and dipole-dipole interaction (the anisotropic interaction) are 35% and 55% larger than the experimental values, respectively.

Stirling[5] constructed a periodic a-SiO_2/Si(111) interface model and calculated the hyperfine parameters of P_b defects. The isotropic interaction (A_{iso}) obtained by the traditional calculation method is 20% higher than the experimental results, and the anisotropic interaction (A_{ani}) overestimates the experimental value by 30%.

Currently, EPR has been used to determine the H_2 passivation process of P_b-type defects. The study[14] found that at the end of the passivation process there was a interspace hydrogen atom and an antimagnetic defect HP_b.

At about 220 ℃, the P_b center can be passivated by H_2. The reaction equation of the passivation reaction is: $P_b + H_2 \rightarrow HP_b + H$, and the reaction barrier for this reaction is 1.66 eV[14]. In a follow-up research[15], Rashkeev proposed that only H^+ not only can easily migrate to the interface but also can stably exist at the interface. Therefore, threefold-coordinated Si can be depassivated by H^+: $Si\text{-}H + H^+ \rightarrow D^+ + H_2$ at about 550 ℃. Subsequently, Brower et al. proposed the process of passivation and depassivation of P_b defects and H atoms The reaction equations are: $P_b + H^0 \rightarrow P_bH$ and $P_bH + H^0 \rightarrow P_b + H_2$. The study suggested that these two reaction processes can proceed spontaneously at room temperature without reaction barriers[16].

Although the process of passivation and depassivation, energy change, and charge distribution of interface have been studied, most of the studies are simulated cluster models or abrupt interfaces. However the structural parameters of the crystal

interface transition are quite different from the amorphous interface which is closer to the actual model. Moreover, for the passivation and depassivation of P_b defects at the a-SiO_2/Si(111) interface, there has been no research and analysis on the intermediate state of passivation and depassivation and its corresponding system energy changes.

In this paper, using molecular dynamics method, based on a-SiO_2 and crystalline Si, Large-scale Atomic/Molecular Massively Parallel Simulator (LAMMPS) software[17-20] is used. In addition, ReaxFF force field[17] is used to construct the a-SiO2/Si(111) interface model by heating, melting and annealing the interface model. Moreover, the rationality of the model is analyzed from the following aspects, such as the bond length and angle distribution of the model, the density of the interface transition region, and the change of Si atoms in different oxidation states along the interface normal direction.

Based on the above-mentioned reasonable model, the basic properties of the amorphous interface defects are studied. The hyperfine parameters of the Pb defect and the g tensor were calculated by using the Gauge Including Projector Augmented Waves(GIPAW) module of the Quantum-Espresso software[21]. And the spin charge density of Pb defects are calculated with Vienna Ab initio Simulation Package(VASP) software[22].

In order to study the reaction process between the Pb defect at the interface and the passivation and depassivation of H, the density functional theory (DFT) is used to construct the initial and final states of the reaction, the climbing image nudged elastic band (CI-NEB) method is used to obtain the reaction curve and reaction barrier[23]. In conclusion, the defect and its process of passivation and depassivation in the a-SiO2/Si(111) interface has been studied by using first-principles calculation.

1 Method

1.1 Molecular Dynamics method

The Molecular Dynamics method (MD method) is an important method for studying the structure and properties of molecular systems. Considering that SiO_2/Si is composed of a Si substrate, a sub-oxidized region, and a SiO_2 region[9], a contact oxidation method can be used to construct a SiO_2/Si(111) interface model. The MD method can impose macroscopic constraints on the system to simulate different systems during the simulation process. In this work, we use molecular dynamics method, use LAMMPS software and ReaxFF force field, to build the a-SiO_2/Si(111) interface model by heating, melting and annealing the interface model.

At first, a-SiO_2 is obtained by melting and quenching a α-cristobalite with 216 atoms. And then, the crystalline Si structure is cleaved to obtain a 8-layers-Si(111) surface. Then, the a-SiO_2 layer is stacked on the Si(111) surface, and the distance between a-SiO_2 and Si is 2 Å. Finally, through the ReaxFF force field in Large-scale Atomic/Molecular Massively Parallel Simulator (LAMMPS) software, we use MD method to anneal the a-SiO_2/Si(111) interface model obtained above. During the annealing process, the interface model is heated from 0 ~1 000 K at a rate of 67 K/ps, and heat treatment is performed at 1000 K to relax the model at that temperature by 50 ps. Cooling down from 1000~ 0 K after passing through the above process, a 13.30×15.36×49.39 model is built.

1.2 First-Principles calculattion

Vienna ab initio simulation package (VASP)[22]

can investigate the electronic structure of matter. It solves Schrödinger's equation and simulates the properties of matter from the atomic scale. First-principles calculations based on Density Functional Theory (DFT) can be applied to systems with a large number of atoms. Nuclei and electrons are considered in this method, so the properties of the system including electrons and magnetism can be obtained.

Therefore, based on the density functional theory (DFT), VASP software is used to perform first-principles calculations by using the Perdew-Burke-Ernzerhof (PBE) in generalized-gradient approximation (GGA)[24]. Furthermore the projector augmented-wave method (PAW) [25] is used to describe the interaction between valence electrons and ion nuclei. In the input file, the plane fundamental cutoff energy is set to 400 eV. Since the unit cell has 353 atoms, in order to make reasonable use of computing resources, we choose one gamma point in the Brillouin-zone integration. When the total energy difference is less than 10^{-5} eV during the calculation, the structure relaxation is completed when the force of the ion relaxation motion is less than 0.05 eV/Å. In order to study the magnetism of unpaired electrons and the spin charge density in the system, the ISPIN parameter is set to 2 in the calculation.

1.3 CI-NEB

The CI-NEB method[23] makes some improvements based on the NEB method. Compared with the NEB method, it can use fewer intermediate images and find more accurate saddle points[23]. Therefore, in order to find the reaction curve and reaction barrier during the passivation or depassivation of P_b-type defects, we use the CI-NEB method to search the minimum energy path (MEP) to find the exact saddle point, and finally obtain the transition state structure. First, we construct the stable initial and final structures, and then insert the appropriate number of images based on the difference between the initial and final structures. In the input file, the label LCLIMB is set to TRUE, and the error of total energy is set to 10^{-5} eV, besides the force on each atom is less than 0.05 eV/Å. Therefore, we can get the reaction curve and reaction barrier in the calculation results by using NEB method.

1.4 GIPAW

Gauge including projector augmented wave (GIPAW)[21, 26-27] method can be approached to the calculation of the all-electron magnetic response by using pseudopotentials, and provide reliable hyperfine parameter for various defects in different semiconductors. This method has been considered by many researchers as a feasible and effective method for calculating hyperfine parameters.

We use the GIPAW method of Quantum-Espresso (QE) software to calculate the EPR hyperfine parameters and g tensor of defects[21].

2 Result and discussion

2.1 The properties of interface model

2.1.1 Interface model

The process of constructing the a-SiO_2/Si(111) interface model is described as above. At an oxidation temperature of 1 000 K, the O atoms in a-SiO_2 will diffuse into the Si layer gradually, and the transition region is formed.

Fig. 1 depicts the distribution of silicon atoms in different oxidation states along the interface normal direction. The valence ratio of Si atoms is

Si^{1+}:Si^{2+}:Si^{3+}=15:22:7. For the transitional region, Si^{1+} is the majority on the side closed to the Si layer, while Si^{3+} is the main oxidation state on the side near SiO_2. The oxidation state distribution and the thickness of the transition region are consistent with the results of X-ray photoelectron spectroscopy[28-29].

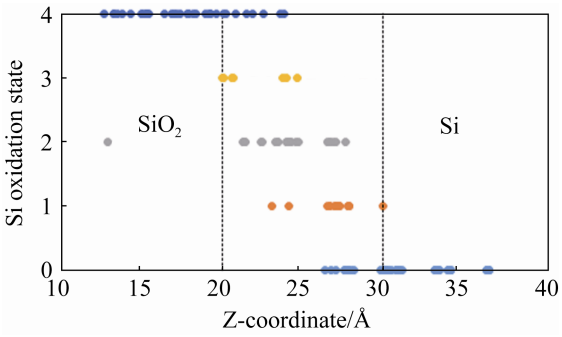

Fig. 1 Distribution of oxidation states of Si along interface normal direction

2.1.2 Distribution of bond length and bond angle

It can be inferred from Tab. 1 that the Si-O bond length in the transition region of the SiO_2/Si(111) interface is slightly larger than that of the bulk, which is consistent with previous studies[30-31]. The oxidation state of the Si is related to the electrostatic attraction between the atoms, so the higher the oxidation state is, the greater the interactions between the atoms is. In addition, the Si(111) plane of the crystal does not match the a-SiO_2 precisely, resulting in internal compressive strain in the a-SiO_2, the ∠Si-O-Si in the transition region in this interface model is sharper than the bulk. At the same time, the ∠O-Si-O in the transition region of this interface model will be slightly lower than that of the bulk because of the existence of the suboxidized Si, which is in line with the change trend of literature[32]. The Si-O bond is repelled due to the interaction between atoms, making the angle ∠O-Si-O of the latter slightly smaller than sp^3 which bond angle is 109°28′.

Tab. 1 Distribution of bond length and bond angle for a-SiO_2/Si(111) interface

Research Data	Si-O(Å)		∠Si-O-Si		∠O-Si-O	
	Transition	Bulk	Transition	Bulk	Transition	Bulk
Exp.	---	1.61	139°–143°	147°–151°	---	109.4°
Theory	1.65	1.64	140.9°	143.0°	106.4°	109.5°
This work	1.66	1.64	140.18°	140.32°	109.17°	109.5°

2.1.3 Plane displacement of Si atoms near the interface

Due to the lattice constants of a-SiO_2 and Si cannot be precisely matched, irreversible stress will be generated at the interface, which will cause a certain displacement of the Si atoms near the interface. As Fig. 2, the average offset of the first layer of Si atoms is 0.474 Å, and the standard deviation is 0.275 Å. The fourth layer of Si atoms has an average offset of 0.251 Å and a standard deviation of 0.044 Å. The calculation results obtained in this paper are consistent with the research results in previous study[33].

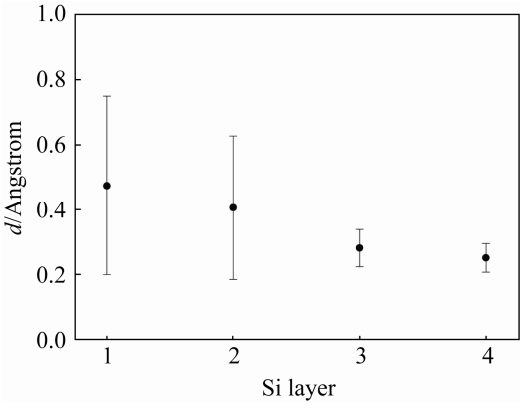

Fig. 2 Plane shift of four Si atoms near interface

2.2 The properties of P_b defect

In order to construct a dangling bond defect which is perpendicular to the [111] direction in the SiO_2/Si(111) interface model, an O atom is removed at the interface, and the dangling bonds on the a-SiO_2

side are terminated with H atoms. The H atom has an effect on the defect, so the H atom is directed to the side away from the P_b defect. The defect model is shown in Fig. 3.

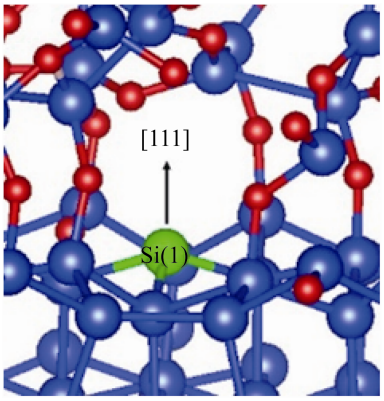

Fig. 3 Structure of P_b defect which defect center atom Si(1) is marked in green

The calculated g tensors and hyperfine parameters by using the GIPAW method are shown in Tab. 2. By diagonalizing the g tensor matrix, three g-value components along different directions which are orthogonal to each other are obtained: g_1, g_2, and g_3 respectively. Besides, from the matrix diagonalization results and Tab. 3, we can see that $g_1=g_{//}=2.005\ 7$, $g_{\perp}=(g_2+g_3)/2=2.013\ 5$, where $g_{//}$ is along the direction of the Si dangling bond, while $g_{\perp}$ is perpendicular to the direction of the P_b defect. Similarly, the hyperfine parameters include the hyperfine parameters $A_{//}$ which are parallel to the direction of the Si dangling bond and $A_{\perp}$ which are perpendicular to the direction of the threefold-coordinated silicon atom. These two parameters are derived from the diagonalization of the hyperfine parameter matrix.

As shown in Tab. 2, the $A_{//}$ obtained in this paper is approximately 14.5% larger than the experimental value, and the $A_{\perp}$ is approximately 6% smaller than the experimental value. However, the $A_{//}$ calculated by the traditional method is 17.8% larger than the experimental value, and the $A_{\perp}$ is about 39% larger than the experimental value. In summary, compared with the traditional PAW method using the GIPAW method, the calculated tensor and hyperfine parameters are more accurate to with the experimental values.

The static charge calculation of the P_b defect structure is performed to obtain the spin charge distribution of the P_b defect (Fig. 4(a)). It can be seen in Fig. 4(a) that the spin charge is mainly distributed near the defect center Si atom (Si(1)) and its three backward Si atoms (Si(2), Si(3), Si(4)). It is shown that these four Si atoms form the structure of •Si≡Si, which is the characteristic atomic structure of P_b defects.

Since the trapping of holes or electrons by P_b defects has an important effect on the silicon-based semiconductor devices, it is necessary to investigate the charged P_b defects. Fig. 4(b) ~ 4(c) show the spin charge distribution after P_b defects trapped electrons and holes, respectively. It can be inferred from Fig. 4 and Tab. 3 that P_b defects are paramagnetism, while negatively-charged P_b^- defects and positively-charged P_b^+ defects are diamagnetism. This feature is consistent with the previous research[34].

Tab. 2 Hyperfine parameters and g tensors of P_b defect

Research Data	$g_{//}$	$g_{\perp}$	$A_{//}$	$A_{\perp}$
	2.001 2	2.008 1	152	89
Exp.	2.001 6±0.0003	2.009 0±0.0003	146.0±5	85.0±8
	2.001 3-2.0017	2.008 7	146	85
Theory	---	---	179.2	123.9
This model	2.005 7	2.013 5	173.7	83.6

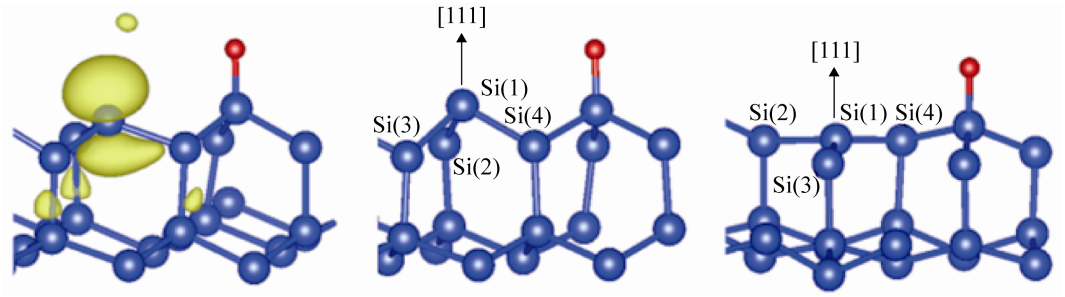

(a) P_b defect (b) P_b^- defect (c) P_b^+ defect

Fig. 4 Spin charge distribution of the charged P_b defect

Tab. 3 Average bond length, tetrahedron parameter t, magnetic moment, and total energy of P_b defects in neutral, negative and positive charge states.

Charged P_b defect	Average bond length/Å	t	Magnetic moment/μ_B	Total energy
P_b	2.286	1.07	1	0(reference)
P_b^-	2.333	2.41	0	+0.733
P_b^+	2.263	0.12	0	–0.056

In order to study the local defect structure, we carry out the quantitative research as follows: average bond length, tetrahedral parameter t, magnetic moment (μB) and the total energy of defect. In addition, the average bond length is that of the defect center Si atom and its three backward Si atoms (Si(1)-Si(2), Si(1)-Si(3), Si(1)–Si(4)). The tetrahedral parameter $t=(360-\sum_1^3 \alpha_i)/31.5$, where α_i is the three bond angles of Si-Si(1)-Si which are formed by the defect center atom and its three backward Si atoms.

The Tab. 3 shows that the average Si-Si bond length of the neutral P_b defect is 2.286 Å, which is slightly shorter than the bond length (2.352 Å) in the Si(111) plane Si of the crystal. On one hand, when P_b defects trap electrons, the average bond length of Si-Si bonds increase by 2% compared to neutral P_b defects, and the total energy of the system increase by 0.733 eV. On the other hand, when P_b defects capture holes, the bond length is shortened by 2.8%, and the total system energy is reduced by 0.056 eV. Moreover, for neutral P_b defects, the average bond angle formed by the defect center Si(1) and its three backward Si atoms is 108.68°, which is very close to the sp^3 structure (the average bond angle is 109.5°). After the P_b defect trap electrons, its Si-Si(1)-Si bond angle is 94.60° on average, which is sharper than that of neutral P_b defects, so the tetrahedral parameter t increase from 1.07 to 2.41. After the holes are trapped by the P_b defect, the corresponding average bond angle is 118.70°, which indicates that the Si-Si(1)-Si bond angle becomes smoother than the P_b defect which is neutral, and the tetrahedral parameter t drops to 0.12 which is close to the ideal sp^2 structure (the average bond angle is 120°).

2.3 Passivation reaction

2.3.1 Passivation reaction between P_b defect and H_2

In order to obtain the initial state of the passivation reaction (Fig. 5(a)), a hydrogen molecule is placed in the void near the threefold-coordinated Si atom. Moreover, a H atom is used to passivate the Si dangling bond, and the other H atom is placed in the interspace near the passivated P_b defect, and we obtain the final state of the reaction (Fig. 5(b)).

As we can see from the Tab. 4, at the beginning of the reaction, the bond length of the hydrogen molecule is 0.748 Å, and the distance between H(1) and Si(1) is 3.496 Å (Fig. 5(a)). In the 01 state (Fig.

6(a)), H(1) gradually approaches the P_b defect, and the distance between H(1) and Si(1) is shortened by 25% compared with the initial state. Besides, the bond length of H(1) and H(2) is 0.755 Å, and the energy of the system increase by 0.2 eV.

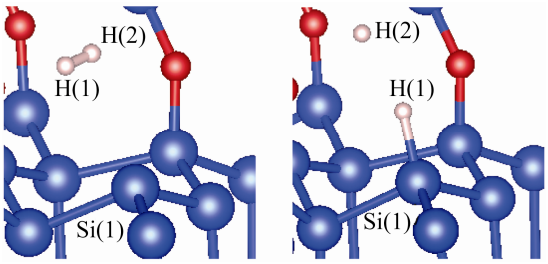

(a) Initial state (00 state) (b) final state (04 state)

Fig. 5 Initial and final state of passivation reaction between H_2 and P_b defect

Tab. 4 Bond length and energy of intermediate state of passivation reaction between H_2 and P_b defect

Bond length and energy	00	01	02	03	04
H(1)-H(2)	0.748	0.755	1.608	2.360	2.631
Si(1)-H(1)	3.496	2.591	1.519	1.491	1.490
Energy/eV	0.000	0.207	1.294	1.218	1.239

Subsequently, the bond between H(1) and H(2) broke, and the distance between H(1) and H(2) increased to 1.608 Å. With the distance between H(1) and Si(1) decreases, H(1) attaches to Si(1) and passivates P_b defect (Fig. 6(b)). At this time, the energy of the system reaches the maximum value of about 1.29 eV (Fig. 7).

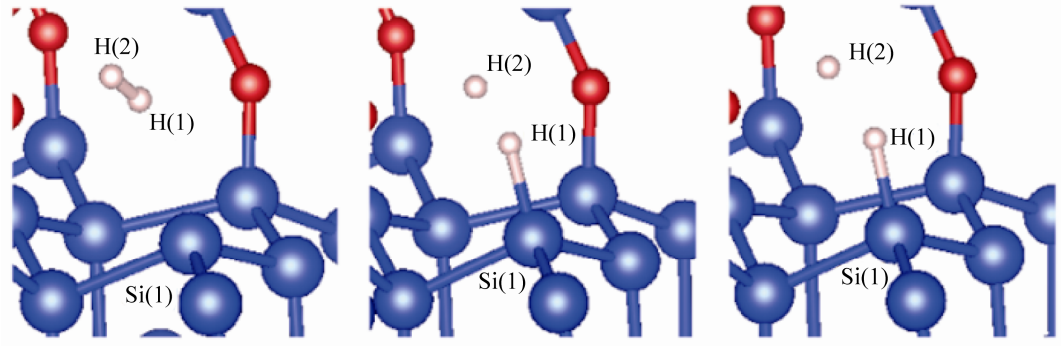

(a) 01 state (b) 02 state (c) 03 state

Fig. 6 Intermediate state of passivation reaction between H_2 and P_b defect

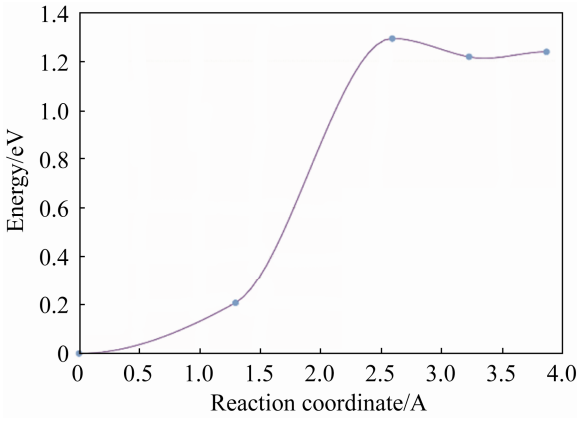

Fig. 7 Energy curve of passivation reaction between H_2 and P_b defects

As the reaction progresses, the structure relaxes, the distance between the two H atoms increases, and the Si(1)-H(1) bond length gradually decreases. When reaching the final state (Fig. 6(c)), the bond length of Si(1)-H(1) is 1.49 Å and the energy of the system is about 1.24 eV, which is consistent with the previous simulation results.

The reason why the final state reaction energy is relatively high is that in the actual passivation reaction, the H atom in the interstitial position is not stable and will still bond with other Si atoms or passivate other dangling bond defects. Subsequent reactions are not considered, which results in higher

end state energy in the simulation.

2.3.2 Passivation reaction between the H atom and P_b defect

In order to construct the initial state of the reaction (Fig. 8(a)), an H atom is added to the interstitial site near the P_b defect. The final state of the reaction (Fig. 8(b)) is obtained by passivation of P_b defect with H atom.

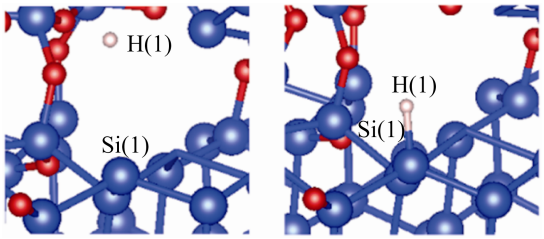

(a) Initial state (00 state) (b) final state (04 state)

Fig. 8 Initial and final state of passivation reaction between H atom and P_b defect

As the Tab. 5 shows that at the beginning of the passivation reaction, the H atom is 3.314 Å away from the Si dangling bond. In the 01 state of reaction (Fig. 9(a)), the distance between H and Si slightly increases, but not so much, so the energy reduction is not obvious.

Tab. 5 Bond length and energy of intermediate state of passivation reaction between H and P_b defect

Bond length and energy	00	01	02	03	04
H(1)-Si(1)	3.314	3.292	2.391	1.614	1.500
Energy/eV	0.000	0.001	–1.308	–3.203	–3.466

As the reaction progresses, H moves toward the P_b defect, and the distance between the H atom and Si dangling bond decrease. Subsequently the distance between H and Si is 2.391 Å, and the energy of the system is –1.380 eV (Fig. 10). With the progress of the reaction, H and Si atoms are bonded. The H(1)-Si(1) bond length is 1.614 Å, which is 32.49% less than that in the 02 state, and the corresponding energy is reduced by 59.16% (Tab. 5).

In the final state of reaction, the Si-H bond length corresponds to the length of the Si-H bond in vacuum. Furthermore, the Si dangling bonds are passivated by H atoms, and the energy of the structure is reduced by 3.466 eV from the initial state. From the reaction curve in Fig. 10, it can be seen that the passivation reaction of H atoms is an exothermic reaction, which is consistent with previous studies[16].

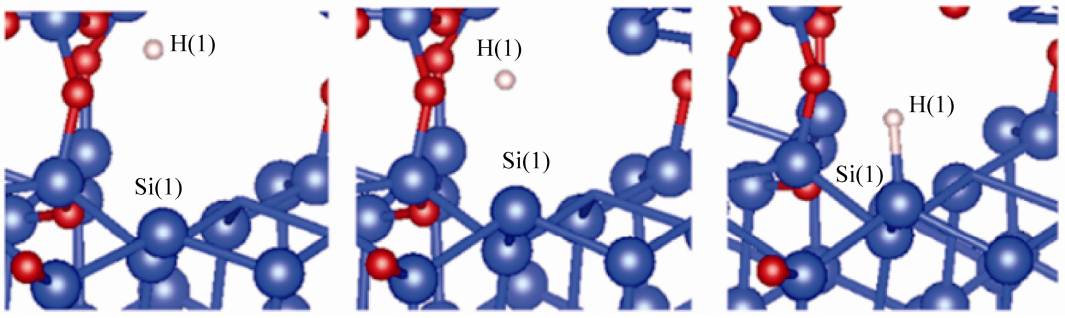

(a) 01 state (b) 02 state (c) 03 state

Fig. 9 Intermediate state of passivation reaction between H atom and P_b defect

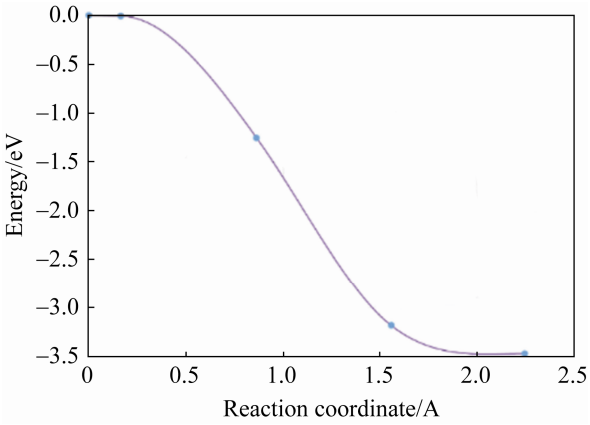

Fig. 10 Energy curve of passivation reaction between H_2 and P_b defects

2.4 Depassivation reaction

2.4.1 Depassivation reaction between proton (H^+) and P_b defects

As can be seen from Fig. 11(a), the silicon hanging bond is passivated by H atom, and a H atom is connected to O(1) atom near the hanging bond Si(1). By subtracting an electron from the system, the initial structure (Fig. 11(a)) of the reaction is constructed. In order to build the final state (Fig. 11(b)), a hydrogen molecule is put into the interspace near the P_b defect, and an electron is also subtracted from the system in the relaxation. It is worth noting that during the entire simulation process, in order to make the initial state and final state charge the same, one electron will be subtracted from the system for CI-NEB calculation.

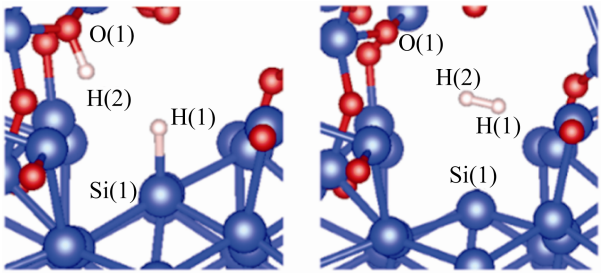

(a) Initial state (00 state) (b) Final state (04 state)

Fig. 11 Initial and final state of depassivation reaction between H^+ atom and P_b defect

In the initial state of the passivation reaction, the bond lengths of Si(1)-H(1) and O(1)-H(1) between H(1), H(2) and silicon and oxygen atoms are 1.507 Å and 0.990 Å, respectively. In the 01 state (Fig. 12(a)) of passivation reaction, the distance between H(1) and H(2) gradually decreases, while the bond length of H(1)-Si(1) and H(1)-O(1) increases to 1.524 Å and 0.997 Å respectively, which is smaller than that of the 00 state. Therefore, the energy of the 01 state is only about 0.005ev higher than that of the 00 state (Tab. 6). It can be seen from Fig. 12(b) that due to the attraction of the interaction between atoms, the distance between H(1) and H(2) is reduced to 0.965 Å, which is 48.42 % lower than that of the state of 01.

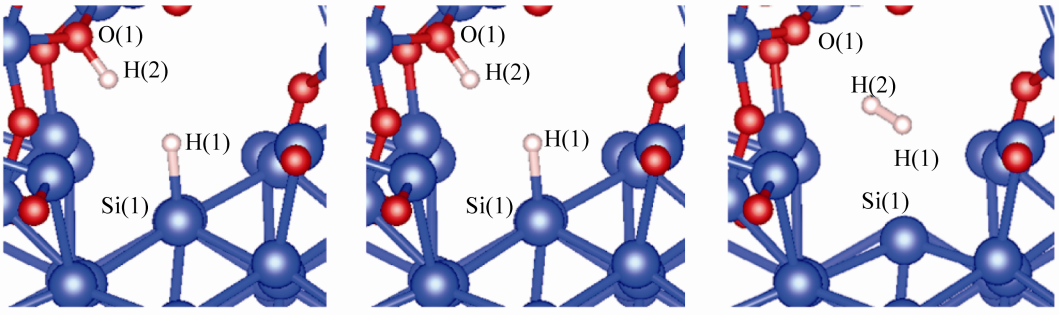

(a) 01 state (b) 02 state (c) 03 state

Fig. 12 Intermediate state of depassivation reaction between H^+ atom and P_b defect

Tab. 6 Bond length and energy of intermediate state of depassivation reaction between H^+ and P_b defect

Bond length and energy	00	01	02	03	04
H(1)-H(2)	2.362	1.871	0.965	0.767	0.759
Si(1)-H(1)	1.507	1.524	1.763	2.231	2.523
O(1)-H(1)	0.990	0.997	1.397	2.169	2.731
Energy/eV	0.000	0.005	0.658	0.224	0.117

On the other hand, as the distance between H(2) and O(1) increases, the proton detach from O(1) and become H atoms in the void. In this process, the energy of the system increases by about 0.65 ev (the energy of protons detonate from O atoms is about 0.55 eV[15], and the energy of the system reaches the maximum (Fig. 13). With the progress of passivation reaction, the distance between H(1) and Si(1) gradually increases.

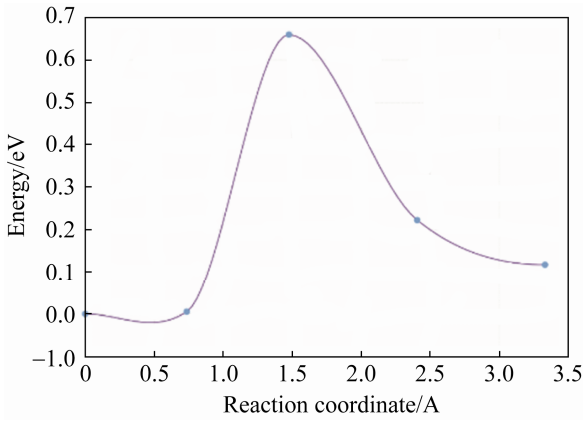

Fig. 13 Energy curve of depassivation reaction between H_2 and P_b defects

From Fig. 12(c), we can see that the distance between H(1) and Si(1) increases from 1.763 A in the state of 02 to 2.23 A, and H(1) is separated from Si(1) atoms. At this time, H(1) forms A bond with H(2), and its bond length is 0.767 Å. The energy of the system is reduced by 66.15% compared with the 02 state, and the system gradually tends to be stable. At the end of the depassivation reaction (Fig. 11(b)), a positively charged P_b defect is formed, as well as a hydrogen molecule in the interstitial space (bond length of 0.759 Å). As can be seen from Tab. 6, the final system energy is 0.117 eV.

2.4.2 Depassivation reaction between H atom and P_b defects

In the initial state of reaction (Fig. 14(a)), a H atom is placed in the interspace near the passivated P_b defect, and the distance between the two H atoms is about 2.6 Å, the bond length of H(1)-Si(1) is 1.5 Å (Tab. 7).

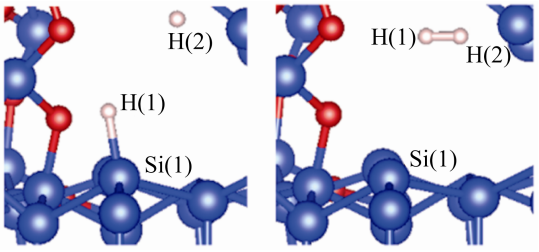

(a) Initial state (00 state) (b) final state (04 state)

Fig. 14 Initial and final state of depassivation reaction between H atom and P_b defect

Tab. 7 Bond length and energy of intermediate state of depassivation reaction between H and P_b defect

Bond length and energy	00	01	02	03	04
H(1)-H(2)	2.601	2.267	1.750	0.760	0.751
Si(1)-H(1)	1.500	1.501	1.518	2.514	3.314
Energy/eV	0.000	0.003	0.025	−1.109	−1.195

As the reaction proceeds, H(1) and H(2) slowly approach each other, while the bond length of H(1) and Si(1) gradually increases. The reaction reaches the 02 state (Fig. 15(b)), at this time, the energy of the system begins to decrease, and heat is released during the reaction. When the distance between H(1) and Si atoms reaches 2.5 Å (Fig. 15(c)), H(1) and H(2) form a bond with a bond length of 0.76 Å. Furthermore, the energy of the system decreases sharply and the structure gradually tends to steady state (Fig. 16).

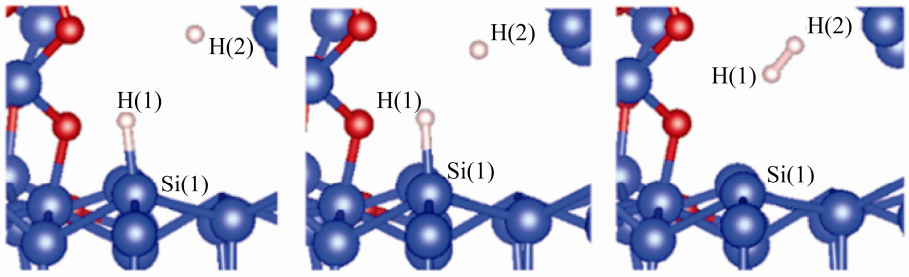

(a) 01 state (b) 02 state (c) 03 state

Fig. 15 Intermediate state of depassivation reaction between H atom and P_b defect

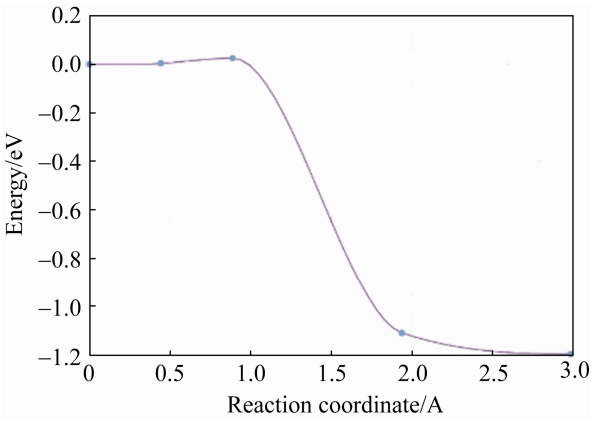

Fig. 16 Energy curve of depassivation reaction between H atom and P_b defects

Finally, in the final state of the reaction (Fig. 14(b)), H (1) is 3.31 Å away from the threefold-coordinated Si atom, and H(1)-H(2) is 0.75 Å. At this time, the energy of the entire system is lowest. In the process of passivation of P_b defects by H atoms, there is no reaction barrier, and the reaction is an exothermic reaction[16], releasing energy of about 1.19 eV (Fig. 16).

3 Conclusion

First, based on MD method and first-principles, an a-SiO_2/Si(111) interface model is constructed. The parameters of the model are basically consistent with previous experimental and theoretical values.

Secondly, based on the above-mentioned reasonable model, the basic properties of amorphous interface defect (P_b defects) is investigated. The various properties of P_b defects are analyzed. According to the conclusion of the analysis, we believe that P_b defects are magnetic, while P_b^- defects and P_b^+ defects are diamagnetic, which is consistent with previous studies.

Finally, CI-NEB method is used to study the passivation and depassivation of P_b defects at a-SiO_2/Si(111) interface. The passivation reaction between H_2 and P_b defects has been investigated in this paper. The reaction barrier is about 1.29 eV. At the end of the reaction, the protons are detached from O, the P_b defect is passivated, and an H atom is present in the gap near the defect in the end.

In addition, the reaction of deactivation of P_b defects by protons (H^+) is also studied in this paper. The reaction barrier is about 0.65 eV. At the end of the depassivation reaction, the H atom detaches from the three-coordinated Si atom and a hydrogen molecule is generated in the interspace. Finally, due to structural relaxation, the structure of the P_b defect is similar to that of sp^2.

Moreover, the process of passivation and depassivation of H atom and P_b defects is simulated. According to the simulation results, the reaction has no reaction barrier. The reaction of the H atom to passivate the P_b defect is an exothermic reaction, and the reaction of the P_b defect to be passivated by the H atom is an exothermic reaction.

Reference：

[1] Schwank J R, Shaneyfelt M R, Fleetwood DM, et al. Radiation Effects in MOS Oxides[J]. IEEE Transactions on Nuclear Science (S0018-9499), 2008, 55(4): 1833-1853.

[2] Godet J, Pasquarello A. Proton Diffusion Mechanism in Amorphous SiO_2[J]. Physical Review Letters (S0031-9007), 2006, 97(15) 155901.

[3] Li P, Song Y, Zuo X. Computational Study on Interfaces and Interface Defects of Amorphous Silica and Silicon[J]. Physica Status Solidi-Rapid Research Letters (S1862-6254), 2019, 13(3): 22.

[4] Edwards A H. Theory of the P_b Center at the Si/ SiO_2 Interface[J]. Physical Review B (S2469-9950), 1987, 36(18): 9638-648.

[5] Stirling A, Pasquarello A, Charlier J C, et al. Dangling Bond Defects at Si-SiO_2 Interfaces: Atomic Structure of the P_{b1} Center[J]. Physical Review Letters (S0031-9007), 2000, 85(13): 2773-2776.

[6] Stesmans A. Structural Relaxation of P_b Defects at the (111)Si/SiO_2 Interface as a Function of Oxidation Temperature: The P_b-generation-stress Relationship[J]. Physical Review B (S2469-9950), 1993, 48(4): 2418-2435.

[7] Stesmans A, Nouwen B, Afanas'ev V V. P_{b1} Interface Defect in Thermal (100)Si/SiO_2: ^{29}Si Hyperfine Interaction [J]. Physical Review B (S2469-9950), 1998, 581(23): 15801-15809.

[8] Kato K, Yamasaki T, Uda T. Origin of P_{b1} Center at SiO_2/Si(100) Interface: First-Principles Calculations[J]. Physical Review B (S2469-9950), 2006, 73: 073302.

[9] Helms C R, Poindexterf E H. The Silicon-Silicon-Dioxide System: Its Microstructure and Imperfections[J]. Reports on Progress in Physics (S0034-4885), 1994, 57(8): 791.

[10] Matsuoka T. Identification of A Paramagnetic Recombination Center in Silicon/Silicon-Dioxide Interface[J]. Applied Physics Letters (S0003-6951), 2012, 100(15): 191.

[11] Takahiro, Yamasaki, Koichi, et al. Oxidation of the Si(001) Surface: Lateral Growth and Formation of Pb0 Centers[J]. Physical Review Letters (S0031-9007), 2003, 91: 146102.

[12] Bahramy M S, Sluiter M H F, Kawazoe Y. First-Principles Calculations of Hyperfine Parameters with the All-Electron Mixed-Basis Method[J]. Physical Review B (S2469-9950), 2006, 73(4): 5111.

[13] Cook M, White C T. Hyperfine Interactions of the P_b Center at the SiO_2/Si(111) Interface[J]. Physical Review Letters (S0031-9007), 1987, 59(15): 1741-1744.

[14] Brower K L. Kinetics of H_2 Passivation of P_b Centers at the (111)Si-SiO_2 Interface[J]. Physical Review B (S2469-9950), 1988, 38(14): 9657-9666.

[15] Fleetwood, D. M，Pantelides, S. T，Rashkeev, S. N, et al. Defect Generation by Hydrogen at the Si-SiO_2 Interface[J]. Physical Review Letters (S0031-9007), 2001, 87(16): 165506.

[16] Brower K L, Myers S M. Chemical Kinetics of Hydrogen and (111)Si‐SiO_2 Interface Defects[J]. Applied Physics Letters (S0003-6951), 1990, 57(2): 162-164.

[17] van Duin A C T, Dasgupta S, Lorant F, et al. ReaxFF: A Reactive Force Field for Hydrocarbons[J]. Journal of Physical Chemistry A (S1089-5639), 2001, 105(41): 9396-9409.

[18] Plimpton S, 1995. Fast Parallel Algorithms for Short-Range Molecular Dynamics[J]. Journal of Computational Physics (S0021-9991), 1993, 117(1): 1-19.

[19] Van Duin A C T, Strachan A, Stewman S, et al. $ReaxFF_{SiO}$ Reactive Force Field for Silicon and Silicon Oxide Systems[J]. Journal of Physical Chemistry A (S1089-5639), 2003, 107(19): 3803-3811.

[20] Fogarty J C, Aktulga H M, Grama A Y, et al. A Reactive Molecular Dynamics Simulation of the Silica-Water Interface[J]. Journal of Chemical Physics (S0021-9606), 2010, 132(17): 174704.

[21] Pickard C J, Mauri F. All-Electron Magnetic Response with Pseudopotentials: NMR Chemical Shifts[J]. Physical Review B (S2469-9950), 2001, 63(24): 303-306.

[22] Kresse G, Furthmüller J. Efficient Iterative Schemes for Ab Initio Total-Energy Calculations Using A Plane-Wave Basis Set[J]. Physical Review B (S2469-9950), 1996, 54: 11169-11186.

[23] Henkelman G, Uberuaga B P, Jónsson H. A Climbing Emage Nudged Elastic Band Method for Finding Saddle Points and Minimum Energy Paths[J]. Journal of Chemical Physics (S0021-9606), 2000, 113(22): 9901-9904.

[24] Perdew J P, Burke K, Ernzerhof M. Generalized Gradient Approximation Made Simple[J]. Physical Review Letters (S0031-9007), 1996, 77(18): 3865-3868.

[25] Kresse G, Joubert D. From Ultrasoft Pseudopotentials to the Projector Augmented-Wave Method[J]. Physical Review B (S2469-9950), 1999, 59(3): 1758-1775.

[26] Blöchl P E. Projector Augmented-Wave Method[J]. Physical Review B (S2469-9950), 1994, 50: 17953-17979.

[27] Mauri F, Pfrommer B G, Louie S G. Ab Initio Theory of NMR Chemical Shifts in Solids and Liquids[J]. Physical Review Letters (S0031-9007), 1996, 77(26): 5300-5303.

[28] Lucovsky G, Phillips J C. Bond Strain and Defects at Si–SiO_2 and Internal Dielectric Interfaces in High-k Gate Stacks[J]. Journal of Physics-Condensed Matter (S0953-8984), 2004, 16(44): S5139-S5151.

[29] Diebold A C, Venables D, Chabal Y, et al. Characterization and Production Metrology of Thin Transistor Gate Oxide Films[J]. Materials Science In Semiconductor Processing (S1369-8001), 1999, 2(2): 103-147.

[30] Bongiorno A, Pasquarello A. Atomistic Model Structure of the Si(100)-SiO_2 Interface From A Synthesis of Experimental Data[J]. Applied Surface Science (S0169-4332), 2004, 234(1-4): 190-196.

[31] Bongiorno A , Pasquarello A . Validity of the Bond-Energy Picture for the Energetics at Si-SiO2 Interfaces[J]. Physical Review B (S2469-9950), 2000, 621(24): 16326-16329.

[32] Miyazaki S, Nishimura H. Structure and Electronic States of Ultrathin SiO_2 Thermally Grown on Si(100) and Si(111) Surfaces[J]. Applied Surface Science (S0169-4332), 1997, 113/114: 585-589.

[33] Feldman L C. Atomic Structure at the (111)Si - SiO_2 Interface[J]. Journal of Applied Physics (S0021-8979), 1982, 53(7): 4884-4887.

[34] Lenahan P M, Conley J F. What Can Electron Paramagnetic Resonance Tell Us About the Si/SiO_2 System?[J]. Cheminform (S1071-1023), 1998, 29(50): 2134-2153.